The Type Ia Supernova Rate at $z \sim 0.4$

R. Pain[1,2], I. M. Hook[1,3], S. Deustua[1], S. Gabi[1], G. Goldhaber[1,4],
D. Groom[1], A. G. Kim[1], M. Y. Kim[1], J. C. Lee[1], C. R. Pennypacker[1,5],
S. Perlmutter[1,4], I. A. Small[1], A. Goobar[6], R. S. Ellis[7], R. G. McMahon[7], K. Glazebrook[9],
B. J. Boyle[8], P. S. Bunclark[8], D. Carter[8], M. J. Irwin[8]
(Supernova Cosmology Project)

Received ______________________; accepted ______________________

[1]E. O. Lawrence Berkeley National Laboratory, Berkeley, California 94720

[2]LPNHE, CNRS-IN2P3 and Universités Paris VI & VII, France

[3]Astronomy Dept, UC Berkeley CA94720

[4]Center for Particle Astrophysics, U.C. Berkeley, California 94720

[5]Space Sciences Laboratory, U.C. Berkeley, California 94720

[6]University of Stockholm, Sweden

[7]Institute of Astronomy, Cambridge, CB3 OHA, United Kingdom

[8]Royal Greenwich Observatory, Cambridge, CB3 OEZ, United Kingdom

[9]Anglo-Australian Observatory, P.O. Box 296, Epping, NSW 2121 Australia

ABSTRACT

We present the first measurement of the rate of Type Ia supernovae at high redshift. The result is derived using a large subset of data from the Supernova Cosmology Project. Three supernovae were discovered in a surveyed area of 1.7 square degrees. The survey spanned a ~ 3 week baseline and used images with 3σ limiting magnitude of $R \sim 23$. We present our methods for estimating the numbers of galaxies and the number of solar luminosities to which the survey is sensitive, and the supernova detection efficiency which is used to determine the control time, the effective time for which the survey is sensitive to a Type Ia event. We derive a rest-frame Type Ia supernova rate at $z \sim 0.4$ of $0.82\ ^{+0.54}_{-0.37}\ ^{+0.37}_{-0.25}\ h^2$ SNu (1 SNu = 1 SN per century per $10^{10}\,\mathrm{L_{B\odot}}$), where the first uncertainty is statistical and the second includes systematic effects. For the purposes of observers, we also determine the rate of SNe, per sky area surveyed, to be $34.4\ ^{+23.9}_{-16.2}$ SNe year^{-1}deg^{-2} for SN magnitudes in the range $21.3 < R < 22.3$.

Subject headings: supernovae, rates

1. Introduction

Type Ia supernovae (SNe) may provide one of the best testable distance indicators at high redshifts, where few reliable distance indicators are available to study the cosmological parameters. A direct measurement of SN rates is therefore important in developing systematic programs to find and study such high-redshift SN Ia distance indicators. Supernova rates at high redshift are also important for understanding galaxy evolution, star formation rates, and nucleosynthesis rates. The dependence of the Type Ia SN rate on redshift can be used to constrain models for the progenitors of the SN explosion. For example Ruiz-Lapuente et al (1995) discuss the correlation of Type Ia rate and explosion time with parent population age and galaxy redshift.

Beginning with the discovery of SN 1992bi (Perlmutter et al 1995a), we have developed search techniques and rapid analysis methods that allow systematic discovery and follow up of "batches" of high-redshift supernovae. At the time of this analysis, the search had discovered 7 SNe at redshifts $z = 0.3$ to 0.5 (Perlmutter et al 1994, 1995a, 1995b). We report here our first estimates of the SNe Ia rate at high z based on a subset of this data set. We are currently following a further 11 SNe in the range $0.15 < z < 0.65$ (Perlmutter et al 1995c) but the data collection and analysis of these SNe are not yet complete.

The observing strategy developed for our search compares large numbers of galaxies in each of ∼50 fields observed twice with a separation of ∼3 weeks, thus almost all our SNe are discovered before maximum light. This search schedule makes it possible to precisely calculate the "control time," the effective time during which the survey is sensitive to a Type Ia event. On the other hand, since hundreds of anonymous high-redshift galaxies are observed in each image, it is more difficult than for nearby SN searches to estimate the number, morphological type and luminosity of galaxies searched in a given redshift range.

The method used to calculate the rate can be divided into two main parts: (i) estimation of the SN detection efficiency and hence the control time, and (ii) estimation of the number of galaxies and the total stellar luminosity (measured in $10^{10}\,L_{B\odot}$) to which the survey is sensitive. We have studied our detection efficiency as a function of magnitude and supernova-to-host-galaxy surface brightness ratio using monte-carlo techniques. By comparing galaxy counts per apparent magnitude interval in our images to the study of Lilly et al (1995) we have estimated the number of galaxies in a given interval of redshift and apparent magnitude. The galaxy counts and efficiency studies, together with the number of confirmed SN detections in this set of images yields an estimate of the SN Ia rate at $z \sim 0.4$.

In Section 2 of this paper, we describe the data we have used. Section 3 deals with the determination of the efficiency of the search, and hence the control times. Section 4 covers the method for estimating galaxy counts. In section 5, we derive the Type Ia rate at $z \sim 0.4$; in Section 6, we estimate the systematic uncertainty; and in Section 7 we discuss the results.

2. The Data Set

For this analysis, we have studied a set of 52 similar search fields observed in December 1993 and January 1994. This is the first sizeable data set to arise from the Supernovae Cosmology Project. These images are suitable for a determination of the SN rate since they were obtained under similar conditions with a single camera at one telescope, and therefore form a well-defined, homogeneous set.

The data were obtained using the "thick" 1242×1152 EEV5 camera at the 2.5m Isaac Newton Telescope, La Palma. The projected pixel size is $0.56''$, giving an image area of approximately $11' \times 11'$. Exposure times were 600s in the Mould R filter, and the individual images typically reach a 3σ limit of at least $R \sim 23$mag. Seeing was typically around $1.4''$. The fields lie in the range $2^h < \alpha(B1950) < 14^h$, $\delta(B1950) > -10°$, excluding the galactic plane ($|b| \gtrsim 30°$). Many of the fields were selected due to the presence of a high-redshift cluster ($z \sim 0.4$). Suitable clusters and their redshifts were taken from Gunn, Hoessel & Oke (1986). The effect of the presence of clusters in the survey fields is taken into account in the calculation of the SN rate (see Section 4).

For most fields, two first-look "reference" images were obtained, here called (ref_1, ref_2), and for all fields two second look "search" images ($search_1$, $search_2$) were obtained $2-3$ weeks after the reference images. The useful area of this dataset is defined by the overlap area of the original set of reference images with the second set of search images. The total useful area covered in this study is 1.73 sq deg.

The analysis procedure and method for finding SNe can be summarized as follows. The images were flat-fielded and zero-points for the images were estimated by comparison with E (red) magnitudes of stars in the APM (Automated plate measuring facility, Cambridge, UK) POSSI catalog (McMahon & Irwin 1992).

For the final analysis of the SN light curves for the determination of q_0, the fields containing SNe are re-observed and calibrated using Landolt standards (Landolt, 1992). However, this calibration is not available for all our search fields that do not contain SNe, hence the use of APM calibration for this study. A comparison of APM E magnitudes with CCD R magnitudes shows that $E-R$ has a mean of -0.2 mag and rms 0.2 mag. We therefore applied a 0.2 mag shift to the APM magnitudes. The uncertainty in the rate introduced by the uncertainty in the zero-points is discussed in Section 6.

The search images were combined (after convolution to match the seeing of the worst of the four images) and the combined reference images were subtracted from this, after scaling in intensity. The resulting difference image for each field was searched for SN candidates.

The main selection criteria was that the object must be a 4σ detection on the difference image. The candidate list was filtered by requiring that the object must not move by more than 2 pixels between the two search images (to remove asteroids), and that the object be a 2.5σ detection on the separate difference images (i.e. $search_1 - combined\ ref$ and $search_2 - combined\ ref$). There was no requirement that the candidate be on a visible host galaxy. The remaining candidate SNe on all the images were inspected visually for obvious problems such as very bright stars nearby, bad columns etc., which could affect the photometry. Follow-up photometry and spectroscopy was used to determine the SN type.

In this subset of the search data three SNe were found, with redshifts 0.375, 0.420 and 0.354. Their properties are summarized in Table 1. SN1994H was discovered in a field centered on a cluster (Abell 370). Its host galaxy is at the cluster redshift ($z_{clus} = 0.373$) at a projected distance of 1.1 arcmin. The redshifts were determined from spectra of the host galaxies. For the purposes of this analysis, we assume these are all Type Ia SNe. This is a likely scenario since Type Ia's are the brightest of the SN types, and therefore the most likely to be detected at large distances. The measured light-curves of the three SNe follow the standard Type Ia light-curve template (Leibundgut, 1988). The data, however, could be consistent with unusually bright Type IIL supernovae. Using our previous estimate of one very bright Type IIL SN for ten Type Ia SNe (Perlmutter et al. 1995), we expect only at most 0.3 Type IIL SNe in the sample. This in agreement with our recent discovery of 11 supernovae where ten are consistent with being Type Ia SNe and one with being a type II (Perlmutter et al. 1995c). For SN1994F we also have a spectrum and it is consistent with that of a Type Ia SN at the date of observation. Other spectra we have obtained for the larger sample of SNe discovered in 1994 are also consistent with those of Type Ia SNe. In addition, in this larger sample, one of the SNe for which no spectrum was obtained was in an elliptical host galaxy, a strong indicator of Type Ia identification. A full discussion of the light curves and spectra will be given in a future paper (Perlmutter et al, in preparation).

During re-analysis of the data for the purposes of calculating the rate, another faint ($R = 22.5$) object was found. This candidate SN which was very near detection threshold, had not been classified as a SN at the scanning stage (final visual inspection) during the first analysis. It had, therefore, not been followed but cannot be ruled out as a possible supernova. The object shows a fairly large motion between the two search images (0.5 arcsec, ~ 1 pixel) which indicates that it may be a faint asteroid. Although unlikely, the possibility that the object is a Type Ia SN was taken into account in the systematic uncertainty as discussed in Section 6.

3. Control Times and Detection Efficiencies

A naïve estimate of the control time ΔT is given by the time during which the supernova light-curve is above a given threshold corresponding to the limiting magnitude of the observations. In our case, this significantly overestimates the control time for the following reasons.

The data presented here were obtained with an observing strategy designed to measure q_0 by conducting a search for SNe on the rise (before their maximum light) using a subtraction technique. The signal on the search image must therefore be significantly larger than on the reference image, reducing ΔT from the naïve estimate by approximately a factor of two. In addition, the detection efficiency depends on the host galaxy magnitude, the image quality, the search technique and strongly on the magnitude of the supernova at the detection time.

In this analysis we compute a control time equal to the weighted sum of days during which the SN can be detected, where the weighting is by the corresponding detection efficiency, ϵ. The control time is given by $\Delta T = \int \epsilon(t)dt$, where ϵ is a function of the observed magnitude m_{obs}, which is itself a function of time t relative to maximum, and δt, the time separation of the search and reference images. To account for the z distribution of galaxies in the fields, control times were calculated in bins of z (and host galaxy magnitude). We assumed that SN magnitude as a function of time follows the average of the best-fit, time-dilated and K-corrected Leibundgut Type Ia template light curves. The generalized K correction described by Kim et al. (1996) was used here.

The three light curves we use as example high-redshift SNe have been calibrated using Landolt standards (Landolt, 1992). Since these are observed light-curves, in *apparent* magnitudes, no explicit dependence of our rate result on H_0 or q_0 is introduced at this stage. The control time was computed taking galactic extinction into account for each field separately. The reddening value for each field $E(B-V)$ were supplied by D. Burstein, (private communication, derived from the analysis of Burstein & Heiles, 1982) and were applied to the data assuming $R_V = 3.1$, and $A_R/A_V = 0.751$ (Cardelli et al, 1989).

The detection efficiency ϵ is a complicated function of many parameters. The efficiency as a function of the SN magnitude depends on the quality of the subtracted images (seeing, transmission) together with the detailed technique (convolution, selection criteria) used to extract the "signal" (SNe candidates) from the "background" (cosmic rays, asteroids, bad subtractions, etc). In addition, there is a slight dependence on the host galaxy magnitude. The detection efficiency was calculated using a Monte-Carlo method. A synthetic image was created for every field by adding simulated supernovae to the search images. The reference images were subtracted from the synthetic search images using exactly the same software as used for the supernova search, described in Section 2, and the number of simulated SNe that satisfy the selection criteria was determined. This technique allows us to measure detection efficiencies as a function of supernova magnitude individually for every field, thus taking into account the other parameters mentioned above. The efficiency derived in this way includes the effects of parts of the image being unusable for the SN search, e.g. due to bright foreground stars.

One hundred simulated SNe were placed on each search image, with a range of SN apparent magnitude, host galaxy apparent magnitude and locations with respect to host galaxies. Each simulated SN was generated by scaling down and shifting a bright star from that image, with signal-to-noise ratio greater than 50, from the image being studied. The position relative to the host galaxy was chosen at random from a normal distribution with σ equal to the half width at half maximum of the galaxy. The shift of the scaled bright star to the host galaxy was by an integral number of pixels to maintain the pixelized point spread function. Since noise fluctuations in the sky background strongly dominates the SN photon noise, it was not necessary to add extra Poisson noise to these simulated SNe.

Figure 1(a)-(c) shows the fractional number of simulated SNe recovered, as a function of SN magnitude (at detection) for the three fields in which SNe were found. Figure 1(d) shows the efficiency as a function of relative surface brightnesses of the SN and host galaxy. This last parameter gives an indication of the effect of SN location with respect to the host galaxy. Although this is a small effect, it was taken into account. For a typical field the detection efficiency is over 85% for any added fake stellar object brighter than $R = 22.0$ magnitude (Note that the more recent searches of this project have worked with significantly deeper images).

At this stage we are able to determine the "survey rate" of SN discoveries that a search for Ia SNe can expect to obtain, per square degree. We give the rate in a range of 1 mag in R, centered on the mean peak R magnitude of the 3 SNe found in this search, $R = 21.8$. The survey rate is given by

$$survey\ rate\ (21.3 < R < 22.3) = \frac{N_{SN}}{\sum_i area_i \times \Delta T_i}.$$

where $N_{SN} = 3$ is the number of SNe we found in the 1 magnitude range, and ΔT_i is the control time for field i, computed for a SN with magnitude $R = 21.8$ at maximum. For example a value of $\Delta T_i = 21$ days was found for the field containing SN1994H observed on 1993 December 19 and 1994 January 12, 24 days apart.

We measure a survey rate for $21.3 < R < 22.3$ of $34.4\ ^{+23.9}_{-16.2}$ SNe year^{-1}deg^{-2} (the error quoted is statistical only). In practice this translates to 1.73 SNe per square degree discovered with a 3 week baseline, in data with limiting magnitude (3σ) $R \sim 23$. The total number of galaxies with $R < 23.8$ surveyed in the 52 fields is approximately 32,000.

4. Galaxy Counts

In order to compare the distant SN rate with local equivalents, we need to know the redshifts of the galaxies we have surveyed. We estimate these in a statistical manner using various groups' analyses of galaxy evolution. In this work we use the galaxy counts derived from the analysis of Lilly et al (1995) to estimate the number of galaxies sampled as a function of redshift. We have also carried out the analysis using the galaxy evolution model of Gronwall & Koo (eg Gronwall & Koo 1995) and that used by Glazebrook et al (1995), to give an estimate of the sensitivity of our results to the assumed form of galaxy evolution.

R band counts as a function of redshift were calculated by S. Lilly based on the analysis of magnitude–redshift data obtained in the Canada-France Redshift Survey (Lilly et al, 1995 and references therein). The survey contains ~ 730 galaxies with $17.5 < I < 22.5$. Lilly et al estimate the expected distribution of galaxies with redshift and R band magnitude $N(z, R)$, by extrapolation from the I band data, with the implicit assumption that the galaxy population does not evolve at redshifts outside the limits of the CFRS sample. $q_0 = 0.5$ was assumed for these calculations (the effect of this assumption on the derived SN rate is discussed in Section 6). Since the I band is close to the R band, and the magnitude range of the CFRS sample is comparable to that of our data, this extrapolation is small.

To check that the assumed distribution of galaxies with R magnitude and redshift, $N(z, R)$, give reasonable galaxy counts compared to our data, we have plotted the number of field galaxies classified by the FOCAS software package, as a function of apparent magnitude, on one of the search images that was *not* targeted at a galaxy cluster. The R-band galaxy counts given by the analysis of Lilly et al (1995) integrated over the redshift range $0 < z < 2$ (dash-dotted line) are shown on the same scale, assuming an effective area for this image of 0.03 sq deg (Figure 2).

Many of our search fields were chosen specifically to target high-redshift clusters. For each of these fields, we estimate the number of cluster galaxies by counting galaxies as a function of R magnitude in a box of size 500×500 pixels centered approximately on the center of the cluster as estimated by eye from the images. The counts in a similar box in a region of the image away from the cluster were subtracted from the cluster counts to give the cluster excess counts as a function of R mag. Examples of these distributions are shown in figure 3. Typically a cluster contributes 10% of the galaxy counts on an image. We assign these galaxies to the cluster redshift, and add the cluster contribution to the $N(z, R)$ for that image given by the models.

5. SN Ia Rates

To compare our derived SN rate with local rates, we express the rate in units of SNu, the number of SNe per century per 10^{10} solar luminosities in the rest-frame B band. To calculate the rate we derive the expected redshift distribution of SNe, $N_{exp}(z)$, which is proportional to the observed SN rate, $r_{SN}(1+z)^{-1}$, where r_{SN} is the rate in the rest-frame of the supernovae. The expected distribution is given by

$$N_{exp}(z) = \frac{r_{SN}}{1+z} \sum_R \sum_i N_{gal}(z,R)_i \times L_B(z,R) \times \Delta T_i(z,R)$$

where i runs over all fields, R is the galaxy apparent R magnitude and L_B is the galaxy rest-frame B band luminosity in units of $10^{10}\,\mathrm{L_{B\odot}}$. We then fit the observed redshift distribution to N_{exp} and hence derive r_{SN}. Here it is assumed that the rest-frame rate r_{SN} is constant in the redshift range of interest ($0.3 \lesssim z \lesssim 0.5$). The control times ΔT, in units of centuries, have been calculated for each field in bins of z and R (the size of the bins used is 0.5 mag in R, 0.05 in z). The derived rate corresponds to a mean redshift given by

$$< z >= \int z N_{exp}(z) dz / \int N_{exp}(z) dz$$

To compute the rest-frame B band galaxy luminosities from apparent R magnitudes, we used $B-R$ colors and B-band K corrections (which include the effects of evolution) supplied by Gronwall & Koo (private communication). These are based on the models of Gronwall & Koo (1995), which give the relative proportions in each bin of z and apparent R magnitude of three different color classes of galaxies (defined as 'red' $B-V>0.85$, 'green' $0.6<B-V<0.85$ and 'blue' $B-V<0.6$). Note that the combined color, K and evolution correction is small in the redshift range of interest ($0.3-0.5$) mostly because the observed R band is close to the rest-frame B-band. The appropriate correction for each color class was applied in the proportions given by the model, and the total luminosity of galaxies in that bin was computed. In this calculation $\mathrm{M_{B\odot}} = 5.48$ and $q_0 = 0.5$ were assumed. Table 2 gives the total luminosity in bins of z and R mag.

Figure 4 shows the expected redshift distribution of SNe, $N_{exp}(z)$, as calculated above. The detection efficiency as a function of z, expressed as the mean control time ΔT, averaged over all fields is also shown, as well as the mean galaxy counts weighted by their B- band luminosities. These two mean quantities are shown merely for illustration; they are not used in the calculation of the expected distribution since each field is treated separately and the results combined.

The rest frame supernovae rate r_{SN} at $z \sim 0.4$ was obtained by fitting the redshift distribution of observed SNe to the expected distribution, $N_{exp}(z)$, using a maximum-likelihood fit with Poisson statistics. The mean redshift corresponding to this rate is $< z >= 0.38$. We derive a value for the SN rate of

$$r_{SN}(z = 0.38) = 0.82 \;^{+0.54}_{-0.37}\; h^2 \text{ SNu}$$

where the error is statistical only.

6. Systematic Uncertainties

Because of the small number of SNe in this first sample, the total uncertainty in this measurement is dominated by statistics. We have, nevertheless, estimated the following systematic uncertainties. The sources studied are listed below, and Table 3 summarizes their contributions.

Total Luminosity estimate The total solar luminosity to which the survey is sensitive was estimated using counts for $N(z, R)$, which have statistical uncertainty due to the finite number of galaxies used in the analysis (e.g. ~ 700 in the analysis of Lilly et al, 1995). The statistical uncertainty in the model contributes about $\pm 0.02h^2$ SNu uncertainty in the rate.

In addition, the luminosity estimation depends on the deceleration parameter, since q_0 enters in the galaxy $N(z, R)$ model/predicted counts, the K corrections of Gronwall & Koo (1995) and the luminosity distance used to calculate the galaxy absolute luminosities. To estimate the sensitivity of our result to q_0, we repeated the analysis using versions of the Lilly et al counts and the Gronwall & Koo model which were calculated for $q_0 = 0.0$. This value of q_0 was also used to calculate the luminosity distances. The deceleration parameter does not affect the calculation of control times because the observed light curves are used in this calculation. The total effect is small, and is dominated by the effect on the luminosity distance. Using $q_0 = 0.0$ rather than 0.5 lowers the derived rate by $0.08h^2$ SNu. Similarly increasing q_0 by 0.5 raises the rate by a comparable amount.

The combined uncertainty in the rate due to the luminosity estimate is therefore $\pm 0.09h^2$ SNu

Contribution from clusters Many of our fields contain a known cluster in the redshift range $0.3 - 0.5$. Four of our fields contain visible clusters which do not have known redshifts. To estimate the effect this uncertainty has on the derived rate, we assigned all the unknown redshifts to $z = 0.1$ and in separate analyses assigned their redshifts to $z = 0.7$ and $z = 0.4$ where this search is most sensitive. The effect of changing the assumed z from 0.1 to 0.4 is to decrease the rate by $0.01h^2$ SNu. Similarly changing the assumed redshifts from $z = 0.4$ to $z = 0.7$ lowers the rate by $0.01h^2$SNu. There is also some uncertainty due to the faint cluster galaxies which are not detected on our images, but which could host a detectable SN. We estimate less than a 10% uncertainty in calculating the overall contribution to the galaxy counts from these clusters, giving a contribution of $\pm 0.02h^2$ SNu to the uncertainty in SNe rate.

Extinction Correction The uncertainty from correcting for extinction was calculated following the estimate from Burstein & Heiles (1982) of the uncertainties in deriving the Galaxy reddening. The effect on the rate is small and amounts to $\pm 0.01h^2$ SNu.

APM calibration Although we used measured SN light curves, calibrated with Landolt standards, to calculate the control times, the galaxies were calibrated using the less accurate APM calibration. Errors in the APM calibration of the fields would thus alter the determination of the efficiency as a function of magnitude. This has a sizeable effect on the derived SN rate since at the magnitude of most of our SNe, the detection efficiency varies rapidly with magnitude. We estimated the size of the effect using the current best estimate of ±0.2 mag uncertainty in the APM calibration of our fields; this contributes $\pm0.10h^2$ SNu to the rate uncertainty (in the sense that brighter assigned magnitudes reduces the derived rate).

Efficiency determination Detection efficiencies were determined using a Monte-Carlo simulation which was statistically limited (one hundred fake SNe were added to each image). Also, models were used for the distance of the SN to the host, and the host galaxy magnitude distribution (assumed to be representative of the total galaxy population). Figure 1d shows, however, that the detection efficiency depends only weakly upon the magnitude difference between the host galaxy and the SN and therefore upon the position of the SN on the host and the host magnitude distribution. We estimated less than 5% uncertainty on the efficiency from using these assumptions. Altogether, uncertainties in the calculation of the efficiency amount to $\pm0.08h^2$SNu uncertainty on the rate.

Range of Type Ia SN lightcurves Control times were calculated using a single template lightcurve with a peak brightness calibrated using the mean of the three observed SNe, therefore making the assumption that Type Ia SNe are standard candles. However, the observed rms scatter in peak brightness for Type Ia SNe could be as big as 0.5 mag depending on the sample used (Riess et al. 1995, Vaughan et al, in preparation). A correlation between peak brightness and lightcurve width (Phillips 1993, Hamuy et al. 1995, Riess et al. 1995) can nevertheless be used to reduce the scatter to 0.21 mag or better (Hamuy et al. 1995 Riess et al. 1995). We therefore estimate a one sigma systematic effect on the measured rate assuming that the overall scatter in brightness of 0.5 comes from two independent sources : i) An "intrinsic" scatter of 0.21 mag, independent of lightcuve width. This was estimated by altering the peak magnitude of the template lightcurve by $0.21/\sqrt{3}$ mag which had the effect of changing the rate by $0.07h^2$ SNu. ii) A contribution of 0.45 ($= \sqrt{0.5^2 - 0.21^2}$) mag correlated with lightcurve width. This was estimated by altering the peak brightness by $0.45/\sqrt{3}$ mag and correspondingly the width of the template lightcurve. To do this we used an approximation for the width-magnitude relation, following the "stretch factor" method of Perlmutter et al (1996) which reproduces the results of Hamuy et al (1995) and Riess et al (1995). This changes the rate by $0.18h^2$ SNu. The overall uncertainty due to the intrinsic and calibratable dispersion of Type Ia lightcurves therefore amounts to $\pm 0.19h^2$ SNu on the rate. Note that this is a conservative estimate since magnitude-limited samples give observed dispersions in peak magnitude of ~ 0.35mag as compared to ~ 0.5mag for volume-limited samples.

Scanning efficiency One SN candidate – the faintest – was not followed up (see section 2). If this was indeed a Type Ia event, then the estimate of the rate increases by $0.27h^2$ SNu.

For any assumed galaxy counts, the main contribution to the systematic uncertainty comes from the range of Type Ia SN lightcurves. High-redshift supernovae from ongoing searches, including the recent 11 discoveries of this group, will soon bring down the statistical uncertainty so that the systematic uncertainty will limit the accuracy of high-redshift SNe rate measurements. The sensitivity to the assumed galaxy counts was not included in this estimation and is discussed in the next section. Assuming the Lilly et al counts for $N(z, R)$, we estimate the total systematic error to be $^{+0.37}_{-0.25}$.

7. Discussion

Galaxy counts To test the sensitivity of our result to the galaxy counts, we recalculated the rate using the model of Gronwall & Koo (1995) and that used by Glazebrook et al (1995).

The galaxy counts of Gronwall & Koo were kindly provided by C. Gronwall, and are based on the analysis in Gronwall & Koo (1995). The model is a "passive evolution" model which has been constrained using galaxy counts in various bands, principally B_J, and color and redshift distributions for various ranges of B_J (see Koo, Gronwall & Bruzual, 1993). In determining their model from the data, $H_0 = 50 kms^{-1} Mpc^{-1}$ and $q_0 = 0.5$ were assumed. A non-standard local luminosity function is assumed to minimize evolution required to fit the counts.

The model used by Glazebrook et al (1995) was also used. This model was derived using the local luminosity function of Loveday et al (1992), the morphological mix given by Shanks et al (1984) and K corrections based on spectral templates of Rocca-Volmerange & Guideroni (1988). In determining the model, $q_0 = 0.5$ was assumed. A normalisation $\phi^* = 0.03(h/Mpc)^3$ was used in this analysis.

These models are quite different as can be seen on Figure 6 where a comparison of the R magnitude distribution between Lilly et al. counts and the counts derived from Gronwall & Koo and Glazebrook et al. models show very substantial differences in the redshift range $0.2 < z < 0.6$, where our SN search is most sensitive. The rate we derive using the model of Gronwall & Koo is $1.61^{+1.05}_{-0.73} h^2$ SNu, almost a factor of two higher than the value derived using the Lilly et al counts. Using Glazebrook et al. model, we derive a value for the rate of $1.27^{+0.83}_{-0.57} h^2$ SNu, which differs by 50% from the rate derived using the Lilly et al counts.

Before drawing any conclusion from these results, it should be noted that unlike the galaxy counts derived from the above models, Lilly et al. counts are based on data that are well-matched to our survey in magnitude and redshift range, and only small amount of extrapolation was required in converting from the I to R band. We therefore believe that the large differences between the results reflects uncertainties in the extrapolation of the models of Gronwall & Koo and Glazebrook et al. to match our data set and we did not quote any systematic uncertainty from galaxy counts in table 3.

Host galaxy inclination and extinction The effect of host galaxy inclination on detection efficiency and host galaxy luminosity estimates should be taken into account when calculating supernovae rates. Cappellaro et al. (1993b) and van den Bergh & Tammann (1991) have estimated the inclination correction factors for nearby searches. In this analysis, both the search technique (in our case subtraction of CCD images) and calculation of the galaxies' luminosities were done differently than in most nearby searches, and the effects of galaxy inclination should not be the same.

Galaxy inclination and extinction would reduce both the number of supernovae detected and the galaxy visible luminosity. These effects may therefore partially cancel in the calculation of the rate. A complete analysis of this effect would require modeling of galaxy opacities, which is beyond the scope of this paper. We therefore compare our uncorrected value with uncorrected values for nearby searches, with particular attention to CCD searches.

Consistency check This analysis is based on a subsample of data taken during winter 1994. The larger sample of seven SNe was discovered in approximately double this number of fields in three different periods of data taking. Preliminary analysis of this data show consistency with the results presented here. As a further consistency check we have examined the original data set for SNe which are past maximum light. This was done by subtracting the search images from the reference images (the reverse of the usual method) and searching for positive signal as before. Two possible SNe were found in this way, consistent with the number discovered on the rise. Since we have no further information on whether these are Type Ia SNe or not, they have not been included in our determination of the rate.

Detection efficiencies The study of detection efficiencies as a function of SN magnitude is a key element of this analysis. These detections efficiencies depend upon many parameters and vary widely from field to field. It is therefore essential to carefully and systematically estimate them. The knowledge of these efficiencies will also be very useful for estimating the effects of Malmquist bias on our sample of SNe. This will be particularly important when using the distribution of measured peak magnitudes to estimate q_0. At $z \sim 0.4$, the present mean efficiency curve, applied to a Gaussian distribution of peak magnitude with 0.2 magnitude intrinsic dispersion, would lead to a shift in the derived value of q_0 of approximately 0.1, if not taken into account.

Comparison with Other Measurement This is the first direct measurement of the Type Ia rate at high redshift. In their pioneering work, searching for high redshift Supernovae, Hansen et al. (1989) discovered a probable Type II event at $z = 0.28$ and a Type Ia event at $z = 0.31$ (Nørgaard-Nielsen et al., 1989). No estimates of SN rates were published after the Type Ia discovery, but beforehand they had concluded that their observation was in mild disagreement with an expected number of Type Ia (based on local rates) of $2.2 - 9.2$ (the range indicates the range of determinations of the local rate from Van den Bergh et al, 1987 and Cappellaro & Turrato 1988).

Nearby supernovae rates have been carefully reanalyzed recently (Cappellaro et al. 1993a & 1993b, Turatto et al., 1994, Van den Bergh and McClure, 1994, Muller et al. 1992) using more precise methods for calculating the control times and correcting for inclination and over-exposure of the nuclear regions of galaxies in photographic searches. The rate obtained for Type Ia SNe are now consistent among these groups and vary between 0.2 h^2 SNu and 0.7 h^2 SNu depending on the galaxy types (E, Sa etc., higher rates are found in later type galaxies).

In order to compare these rates with our measurement, one should remember that (1) most local measurements have been based on photographic data rather that CCD data as used here, (2) we did not apply any correction for host galaxy absorption and inclination and (3) at z ~0.4 the ratios of galaxy type are different. Using galaxy counts from Gronwall & Koo in the range $0.35 < z < 0.45$ and $21.75 < R < 22.25$ and their color classification of galaxies (Gronwall, private communication), we estimate the relative fraction of galaxy types in our sample to be 23% E-S0, 15%S0a-Sb and 62% Sbc-Sd. Combining this with the Type Ia rates measured by Cappellaro et al (1993b) for E-S0, S0a-Sb and Sbc-Sd galaxy types, we can calculate the local rate we should find if the mix of galaxies locally were the same as the mix at $z \sim 0.4$. We obtain 0.53 ± 0.25 h^2 SNu. Our measured value of $0.82^{+0.65}_{-0.45} h^2$ SNu (where statistical and systematic uncertainties have been combined), although slightly higher, agrees with this value within the uncertainty and indicates that Type Ia rates do not change dramatically out to z ~0.4. Note, however that correcting for host galaxy extinction and inclination may change this conclusion.

Theoretical estimates of Type Ia SN rates have been derived from stellar and galaxy evolution models. Calculations were done mostly for elliptical galaxy type. Earlier calculations predicted lower than observed rates for Type Ia (Tornambè & Matteucci 1986, 1987, Tornambè 1989). More recent calculations, based on evolutionary models of elliptical galaxies, predict rates of $\sim 0.1 h^2$ SNu (Ferrini & Poggianti 1993). Assuming a factor of ~ 2 higher rate in non-elliptical galaxies compared to ellipticals (Cappellaro et al. 1993b) and a mix of galaxy types as above, we convert this to an overall rate of Type Ia SNe at $z \sim 0.4$ in all galaxy types, and derive a value of $\sim 0.37h^2$ SNu. Our total uncertainty of $^{+0.65}_{-0.45}$ in the measurement presented in this paper does not allow any firm conclusion but our observed rate seems to lie above this theoretical prediction. There may be an increase of Type Ia rate with redshift. Ruiz-Lapuente, Burkert & Canal (1995) predict significant increase in rate for redshifts between 0.4 and 0.8 depending on the specific model they consider. In the near future, our ongoing high-z SN search and others should provide enough data to constrain the theoretical calculations.

Acknowledgments

This work was supported in part by the National Science Foundation (ADT-88909616) and the U.S. Dept. of Energy (DE-AC03-76SF000098). We thank the La Palma staff & observers for carrying out service observations. We also thank Simon Lilly and Caryl Gronwall & David Koo for providing their galaxy counts prior to publication, and Richard Kron for useful discussions. I.M. Hook acknowledges a NATO fellowship. R. Pain thanks Gerard Fontaine of CNRS-IN2P3 and Bernard Sadoulet of CfPA, Berkeley for supporting this work.

Name	z	Host R mag	Dist. from Host Core	Discovery R mag
1994H	0.375	21.1	$1.0''$	21.9
1994al	0.420	21.2	$1.0''$	22.6
1994F	0.354	20.2	$2.8''$	22.0

Table 1: Summary of the three SNe found in the survey data described in the text.

$R\backslash z$	0.05	0.15	0.25	0.35	0.45	0.55
18.5	12.94	824.9	2808	3671	881.4	88.43
19.5	7.942	322.6	2451	5368	3691	2031
20.5	3.799	154.7	943.1	3520	6050	6430
21.5	1.647	87.31	397.2	1281	3059	6699
22.5	1.211	30.60	226.4	587.2	1243	2728
23.5	1.126	11.26	88.16	340.4	744.2	1212
24.5	0.1458	18.56	17.07	105.8	351.5	799.2
25.5	0.00	9.939	60.59	27.68	65.53	280.5

Table 2: Total luminosity in units of $10^{10}\,\mathrm{L_{B\odot}}$ given by the counts of Lilly et al (1995) and assuming $q_0 = 0.5$, in the survey area of 1.73 sq deg. Bin widths are 0.1 in z, 1.0 mag in R, centered on the values shown.

Source	uncertainty
Luminosity estimate	0.09
Cluster contribution	0.02
Galaxy extinction	0.01
APM calibration	0.10
Detection efficiency	0.08
Range of Ia lightcurves	0.19
Scanning efficiency	$-0.00 + 0.27$
Total syst. uncertainty	$-0.25 + 0.37$

Table 3: Systematic Uncertainties. Uncertainties in the rate are in h^2 SNu. All uncertainties were estimated using the Lilly et al counts for the magnitude-redshift distribution of galaxies, N(R,z). Note that no estimate of systematic uncertainties from galaxy counts and from Galaxy inclination and extinction was made.

REFERENCES

Burstein, D., Heiles, C. 1982, AJ, 87, 1165

Cardelli, J. A., Clayton, G. C. Mathis, J. S 1989, ApJ, 345, 245

Cappellaro E., Turatto M. 1988, A&A, 190, 10

Cappellaro E., Turatto M., Benetti S., Tsvetkov, D. Yu, Bartunov, O. S. & Makarova I. J. 1993a, A&A, 268, 472

Cappellaro E., Turatto, M., Benetti, S., Tsvetkov, D. Yu, Bartunov, O. S. & Makarova I. J. 1993b, A&A, 273, 383

Ferrini F. & Poggianti B. 1993, ApJ, 410, 44

Glazebrook, K. Ellis, R. Santiago, B. Griffiths, R. 1995, MNRAS, 275, L19

Gronwall, C. & Koo, D. 1995, ApJ, 440, L1

Gunn, Hoessel, Oke, B 1986, ApJ, 306, 30

Hansen, L., Jørgensen, H. E., Nørgaard-Nielsen, H. U., Ellis, R. S., Couch, W. J. 1989, A&A, 211, L9

Hamuy, M., Phillips, M. M., Maza, J., Suntzeff, N.B., Schommer, R., & Aviles, R. 1995, AJ, 109, 1

Kim, A., Goobar,. A, Perlmutter, S. 1996, PASP, 108, 190

Koo, D., Gronwall, C., Bruzual, A. G. 1993, ApJ, 415, L21

Landolt, A. U. 1992, AJ, 104, 340

Leibundgut, B. 1988, Ph. D Thesis, University of Basel

Lilly, S., Tresse, L., Hammer, F., Cramptopn, D., Le Fevre, O. 1995, ApJ, 455, 108.

Loveday, J. Peterson, B. A., Efstathiou, G. Maddox, S. J. 1992, ApJ, 400, L43

Muller et al. 1992, ApJ, 384, L9

McMahon R. G. and Irwin M. J. 1992 , Digitised Optical Sky Surveys, eds H. T. MacGillivray and E. B. Thomson, Kluwer p 417.

Nørgaard-Nielsen, H. U. et al., 1989, Nature, Vol 339, 523

Perlmutter, S., et al. 1994. IAUC no. 5956

Perlmutter, S., et al. 1995a. ApJ, 440, L41

Perlmutter, S. et al 1995b. IAUC no. 6263

Perlmutter, S. et al 1995c. IAUC no. 6270

Perlmutter, S. et al. 1996 in Proceedings of NATO Advanced Study Institute on Thermonuclear Supernovae, R. Canal, P. Ruiz-Lapuente and J. Isern, Eds., (Kluwer Dordrecht), in press

Phillips, M.M. 1993, ApJ, 413, L105

Riess, A. G., Press, W. H., & Kirshner, R. P. 1995, ApJ, 438, L17

Rocca-Volmerange, B., Guideroni, B. 1988, A&AS, 75, 93

Ruiz-Lapuente, P. Burket, A., Canal, R. 1995, ApJ, 447, L69

Shanks, T. S, Stevenson, P. R., Fong, R., MacGillivray, H. T 1984, MNRAS, 206, 767

Tornambè A. & Matteucci F. 1986, MNRAS, 223, 69

Tornambè A. & Matteucci F. 1987, ApJ, 318, L25

Tornambè 1989, MNRAS, 239, 771

Turatto M., Cappellaro & E., Benetti S. 1994, A. J., 108, 202.

Van den Bergh S. & McClure R. D. 1994, ApJ, 425, 205

Van Den Bergh, S. McClure, R. D., Evans, R. 1987, ApJ, 323, 44

Van Den Bergh, S., Tamman, G. A. 1991, ARA&A, 29, 363

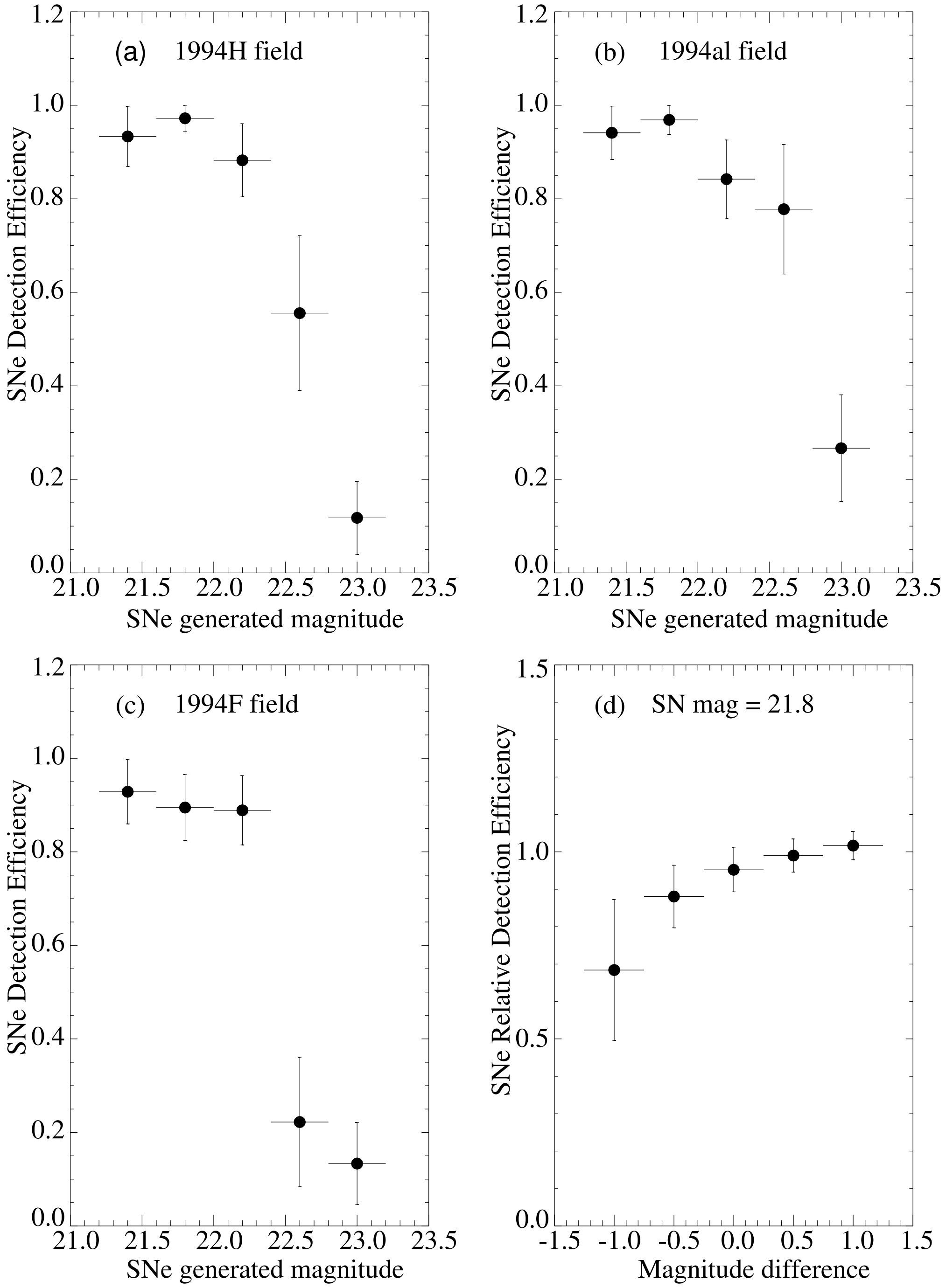

Fig. 1.— (a)-(c) Detection efficiency as a function of magnitude for the three difference images in which SNe were found. The vertical error bars show the 1σ statistical uncertainty, and the horizontal bars show the bin ranges (d) Detection efficiency as a function of relative SN to host surface brightness.

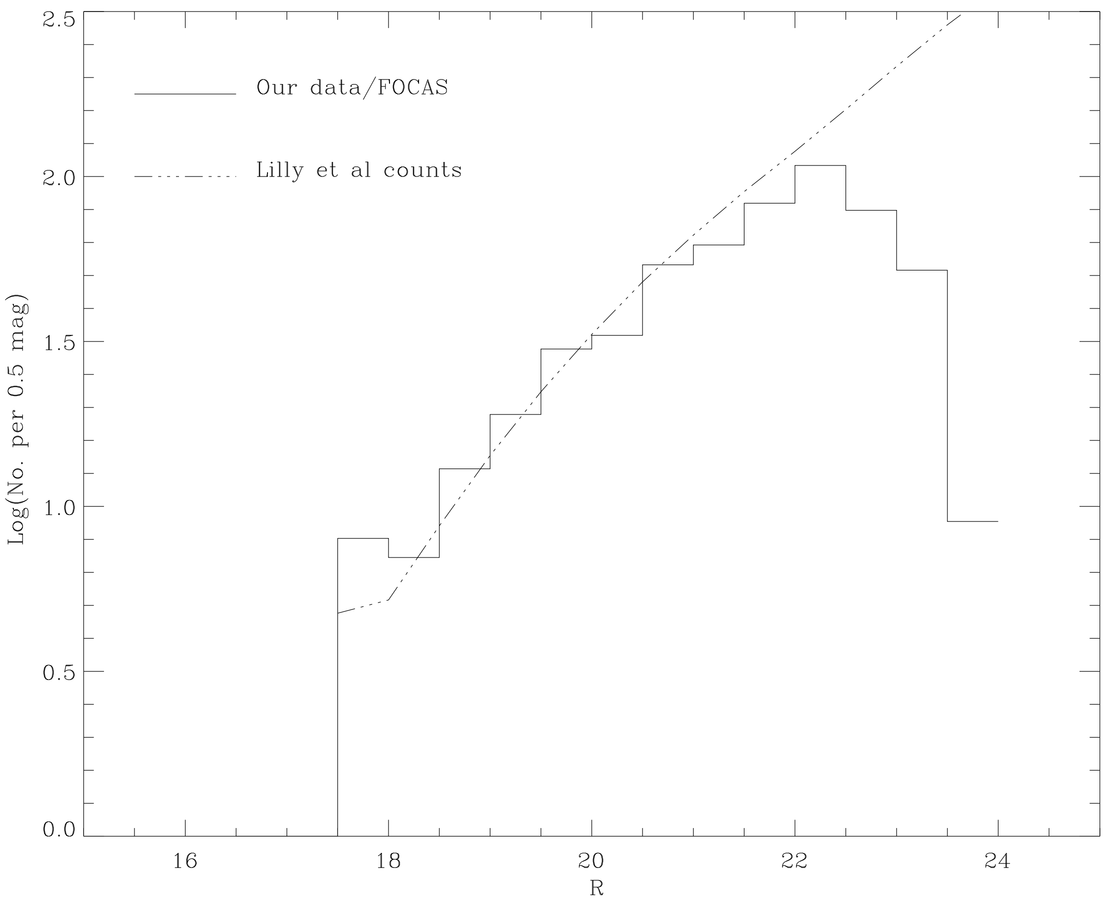

Fig. 2.— Number of galaxies as a function of magnitude determined from one of our non-cluster images using FOCAS. The dashed-dot line shows the counts derived from the analysis of Lilly et al (1995), integrated over the redshift range $0 < z < 2$, and normalized to the image area of 0.03 sq deg.

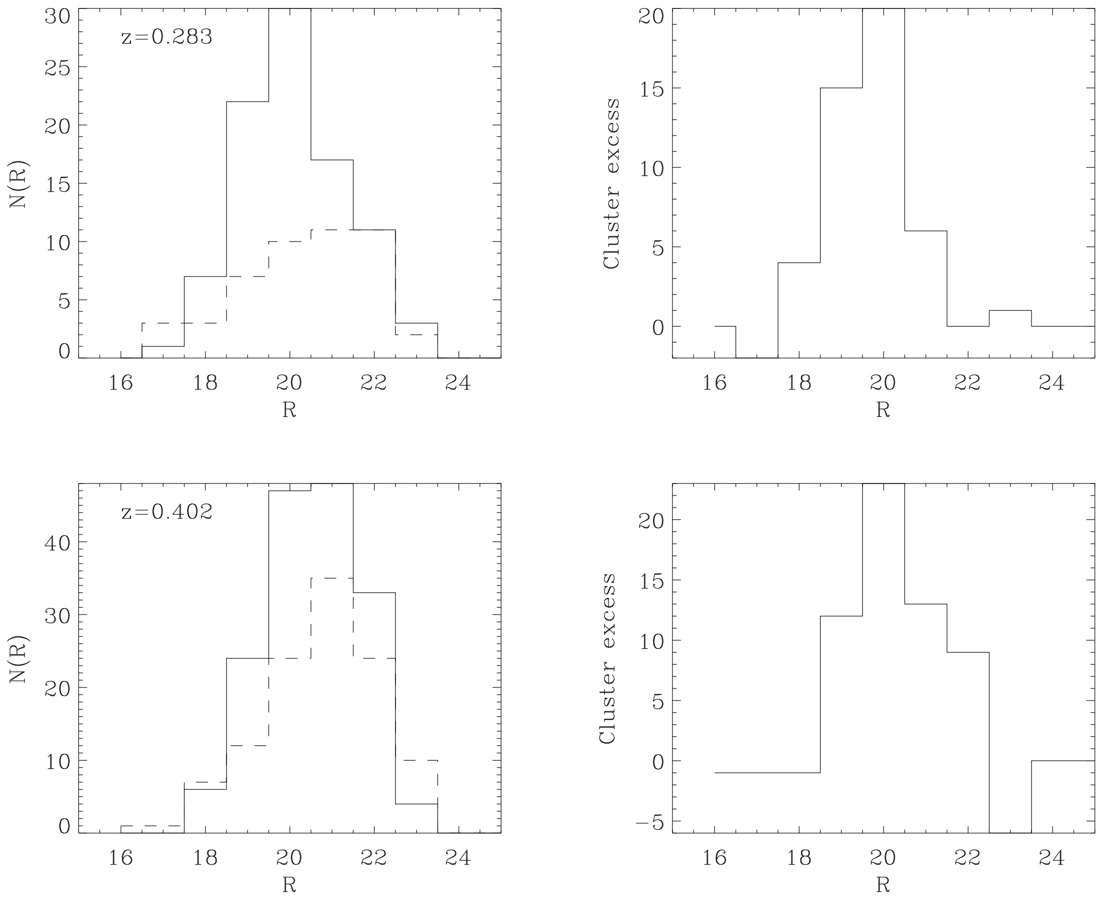

Fig. 3.— Galaxy $N(R)$ in a 500×500 pixel box containing the cluster (solid line) and $N(R)$ in a similar box away from the cluster (dashed line) for two fields. The excess cluster counts are shown in the right hand panels.

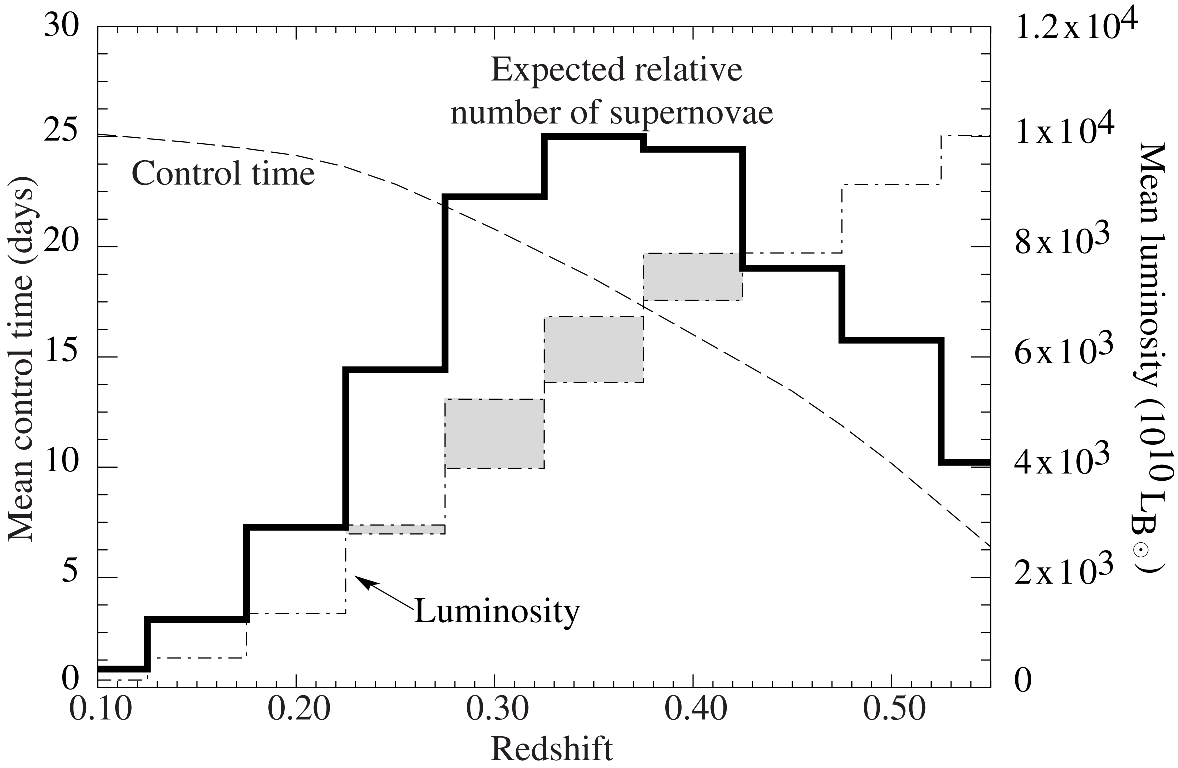

Fig. 4.— The expected number of supernovae as a function of z (solid histogram) together with the overall detection efficiency given as a "control time" (dashed curve) and the luminosity-weighted number of galaxies (dash-dot histogram). The contribution to the luminosity from clusters is shown by the shaded area. The December 1993-January 1994 search was most likely to find SNe with redshifts between $z = 0.3$ and $z = 0.4$. Between $z = 0.3$ and $z = 0.55$, the search was more than 50% efficient. Note that our more recent searches go deeper than this data.

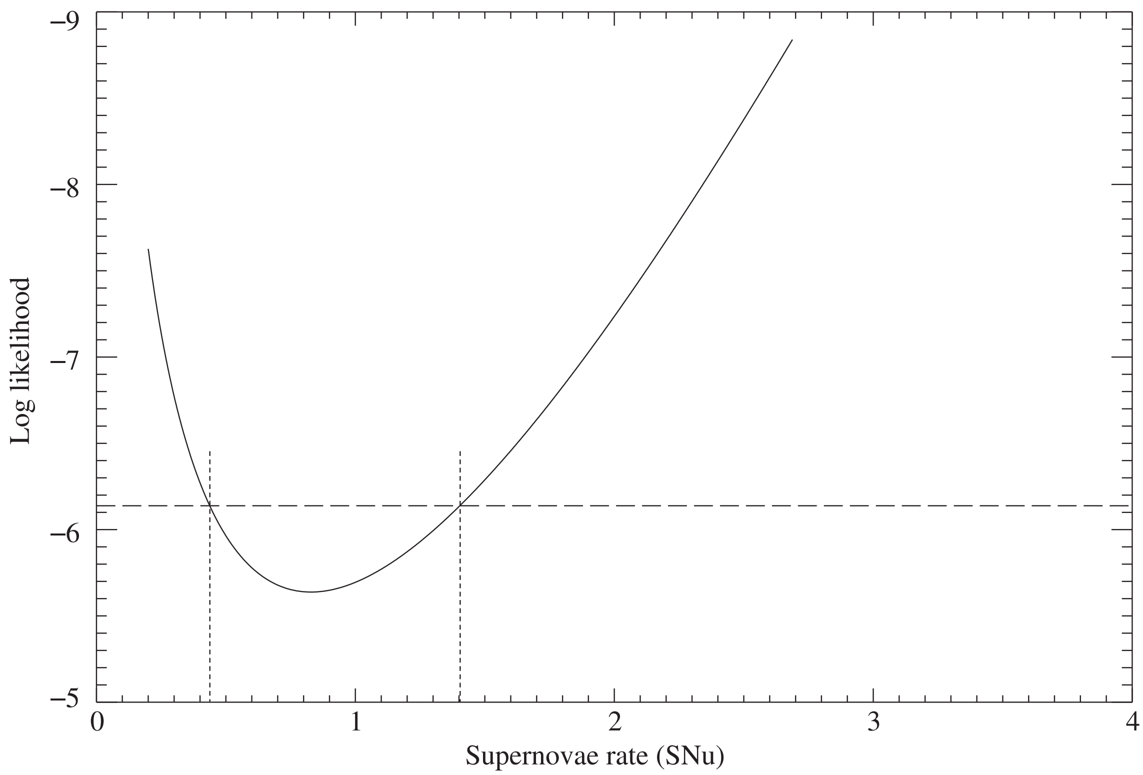

Fig. 5.— Results from the maximum-likelihood fit of the observed distribution of SN events to the expected distribution, $N_{exp}(z)$. The dashed vertical lines show the $\pm 1\sigma$ uncertainty in the result.

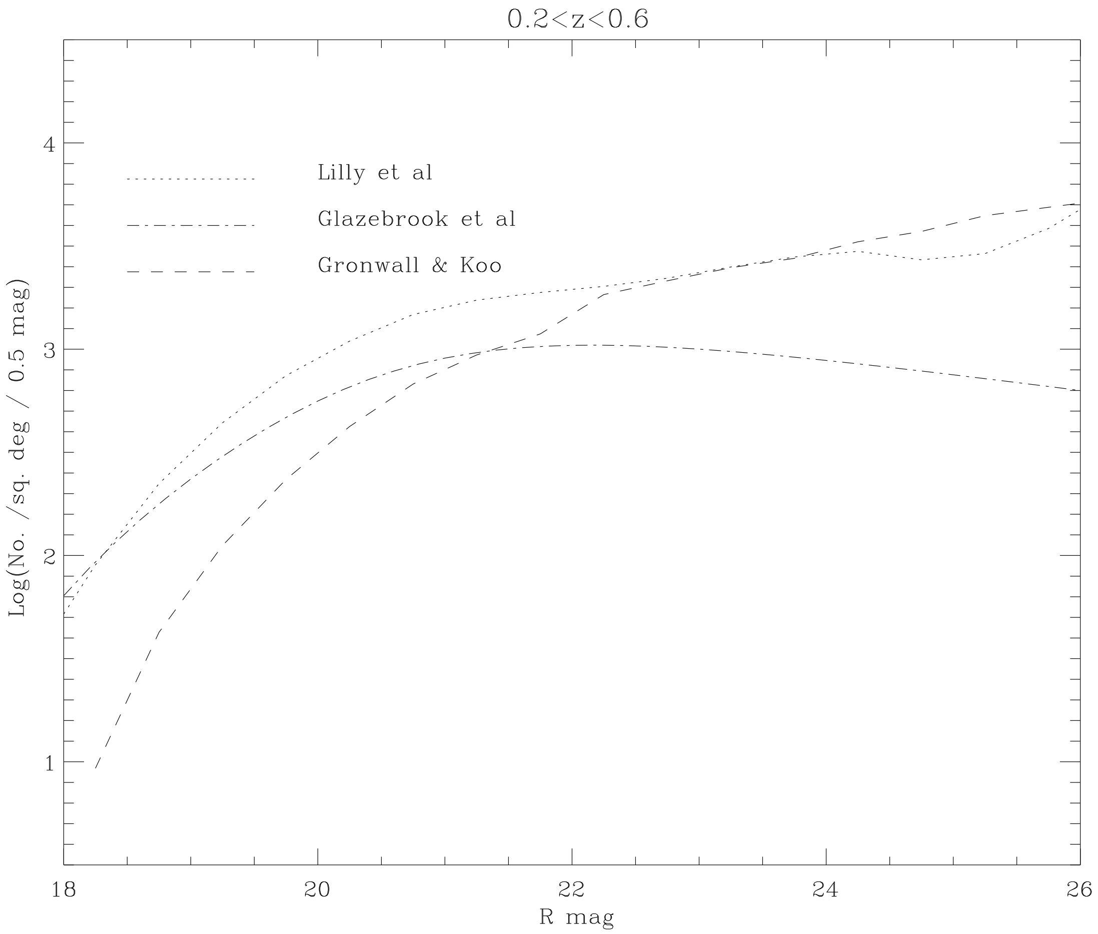

Fig. 6.— Comparison of the galaxy N(R) in the redshift range $0.2 < z < 0.6$. The counts of Lilly et al (derived from the analysis of Lilly et al 1995), and the models of Gronwall & Koo (1995) and Glazebrook et al (1995) are shown. The fluctuations in the curves reflect the statistical fluctuations in the data from which the models were derived.